



## Research Article

# The Development of Data Acquisition System of Formula SAE Race Car Based on CAN Bus Communication Interface and Closed-Loop Design of Racing Car

Zhonghao Li , Da Wang , and Qiao Kang

Jilin University, College of Automotive Engineering, Jilin University, Changchun, China

Correspondence should be addressed to Da Wang; wangda\_gsspeed@jlu.edu.cn

Received 21 June 2021; Revised 13 July 2021; Accepted 23 July 2021; Published 26 August 2021

Academic Editor: Balakrishnan Nagaraj

Copyright © 2021 Zhonghao Li et al. This is an open access article distributed under the Creative Commons Attribution License, which permits unrestricted use, distribution, and reproduction in any medium, provided the original work is properly cited.

This paper is mainly based on the college formula race car, through the application of CAN bus communication interface settings, the layout and adjustment of the car sensors, and then carry out the data collection and analysis of the car. CAN bus is the local area network of controller and is one of the field bus which is put forward by German Bosch company and applied most widely in the world. The development of the data analysis system is mainly based on the MoTeC i2 data analysis software. MoTeC i2 data analysis software has been developed for many years under the continuous research of professional teams all over the world. According to the data analysis requirement of FSAE undergraduate Formula 1 teams, this paper introduces a series of data analysis methods closely related to FSAE, mainly including data channel research. This paper expounds the reliability, suspension, tire temperature, steering, and braking data analysis, respectively. Based on the data analysis template created by Motec i2, this paper conducts analysis and basic application according to the data of the real car, so as to meet the requirements of verifying design made by simulation model and tuning the real car scientifically. By means of wheel speed sensor, acceleration sensor, displacement sensor, multichannel temperature sensor, and so on, we conduct a series of tests on 2020 season car, including endurance test, linear acceleration experiment, steady rotation, etc., evaluate the data collected, and then carry on a reasonable set-up of racing, ultimately improving lap speed.

## 1. Introduction

Formula SAE (FSAE) was first proposed by an American factory in 1978. This race is held for college students to collect small formula cars with creative design and scientific ideas. These cars are stable and durable in all aspects of performance. Compared with foreign countries, our domestic college student formula racing started late. The first Formula Student China (FSC) competition was held at the Shanghai International Circuit in 2010. Formula Student of China (“China FSC”) is a car design and manufacturing competition organized by students majoring in automotive engineering or automotive related in universities. Each participating team in accordance with the rules of the race and racing car manufacturing standards, in one year’s time to design and manufacture a small single-seat recreational racing car in the acceleration, braking, handling, and other aspects of

excellent performance, can successfully complete all or part of the race links. China FSC is committed to building a public platform for the training and selection of outstanding domestic automotive talents, and through general assessments to improve students’ comprehensive capabilities in five aspects, including design, manufacturing, cost control, commercial marketing, communication, and coordination. In order to improve the comprehensive quality of automotive students, make long-term talent accumulation for the development of China’s automotive industry, and promote the strategic direction of China’s automotive industry from a “manufacturing country” to an “industrial power” [1]. Gspeed Electric Racing Team of Jilin University has participated in the FSC series for 5 consecutive years. In 2019, it went to Japan to participate in the Formula Student Japan and won the second prize of design project many times. In 2018, it won the first prize of the FSC. GspeedE-2019 and

GspeedE-2020 race cars are shown in Figures 1 and 2, respectively. When we design a racing car, we often fail to make a reasonable design for some parameters of each system, and the rough design fails to support and prove the completed design with data. Therefore, we installed a data acquisition system on our race car, that is, the sensors we need and the wiring harnesses which connect them to a low-voltage electrical system and panel. Then, we used MoTec i2 to deal with the data we collected. Due to the large proportion of engineering design events and dynamic events in Formula Student [2], data analysis of race cars, which plays an important role in verifying design, guiding tuning, and further contributing to future design, do show its important value. Therefore, we do research on analysis methods of race cars and put it into practice by using MoTec i2 templates and math channels, which quickly analyze the large amount of data generated by each test. In this way, we obtain the direction of tuning and improve the performance of our car.

At the same time, the data acquisition and analysis system of the whole car is a feedback system for driver training and making suggestions for tuning [3]. Through scientific road test and data analysis, the whole process can form a closed-loop design. In addition, the driving habits and styles of different drivers can be summed up by recording and analyzing the same project they conduct. In this way, different car set-up methods can be matched for different drivers. Figure 3 shows the flow chart of data collection and analysis of the race car.

The sensor interface setup and connection of the vehicle are based on CAN bus communication protocol, among which, the car has three CAN communication networks:

- (1) Motor control network, connecting the vehicle controller with the motor controller, to realize the function of sending the torque instruction of the drive system and obtaining the working state of the motor of the drive system
- (2) The conventional information communication network realizes the information transmission between the vehicle controller and the battery management system, instrument panel, sensors, and other equipment
- (3) In order to charge the communication network, the experimental information transmission between the battery management system and the charger

Using the MoTeC C125 racing digital instrument, ECU uses CAN-B to collect and record training data for improved vehicle performance.

Figure 4 shows the CAN bus network of the whole vehicle.

## 2. Reliability Data Analysis

As we know, one of the most important functions of the data acquisition system is to find the potential faults of race car by monitoring the reliability data, which determines whether the car can run normally or not. So we should make obtaining and checking reliability data a top priority. Once anything abnormal is found, stop the car immediately and



FIGURE 1: GspeedE-2019 racecar.



FIGURE 2: GspeedE-2020 racecar.

troubleshoot the fault. For Formula E racing, the important reliability data consist of high voltage battery voltage, high voltage battery temperature, motor output power, low voltage battery voltage, etc. Second, there are some reliability indicators, such as tire pressure, and brake pressure. Figure 5 is the reliability data template.

To check the reliability data, the first step is to observe the maximum and average values of each channel, and the second step is to examine its changing trend. The observation of maximum value can determine whether the data is within safe range, while the observation of variation trend can determine whether the car is running normally during the whole process and can predict the state of the car when running continuously. Especially in endurance test, the data of battery temperature and power usually change linearly.

In order to know the condition of reliability parameters during each run, we set up an alarm mechanism on the car instrument panel. In the endurance race, it is one of the key factors to detect abnormal reliability parameters in advance and make a right decision.

Similarly, an alarm mechanism can be set in the data analysis software to find out the problematic channel data in the first time.

If the voltage provided by the power battery is found to be too low, it is considered that the power supply system of the battery box body has poor contact and the battery module bolts have loosened. At this time, the battery box should be inspected and the battery management system (BMS) should be used for fault detection.

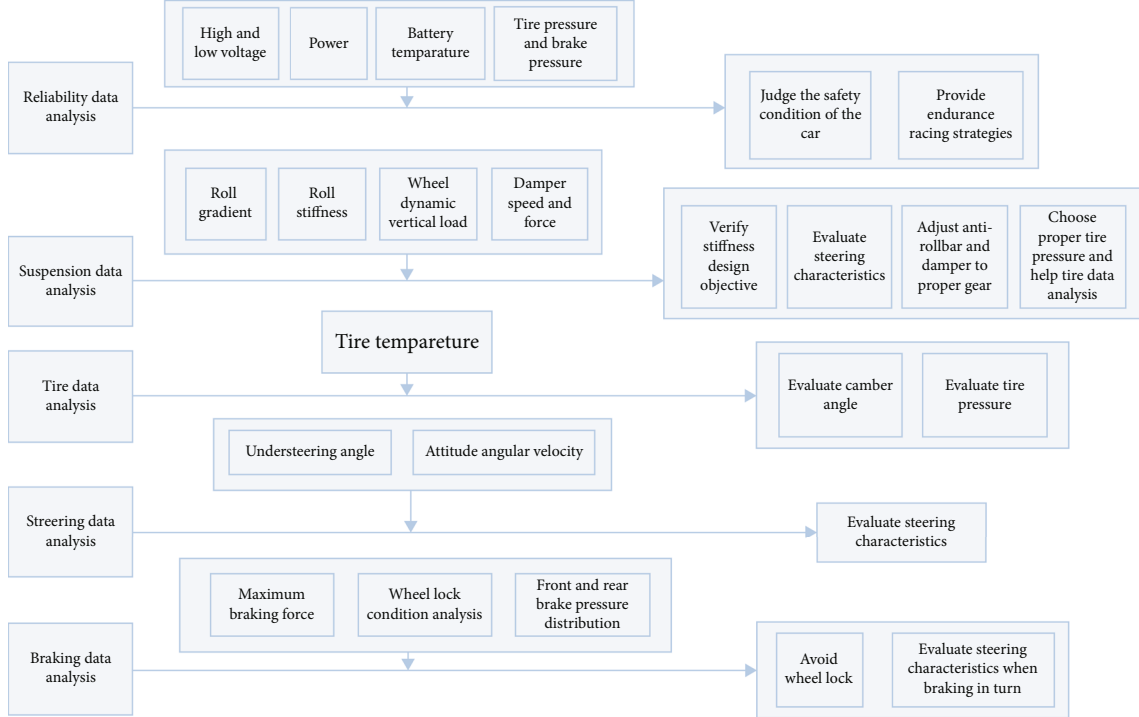


FIGURE 3: Flow chart of data collection and analysis for racing car.

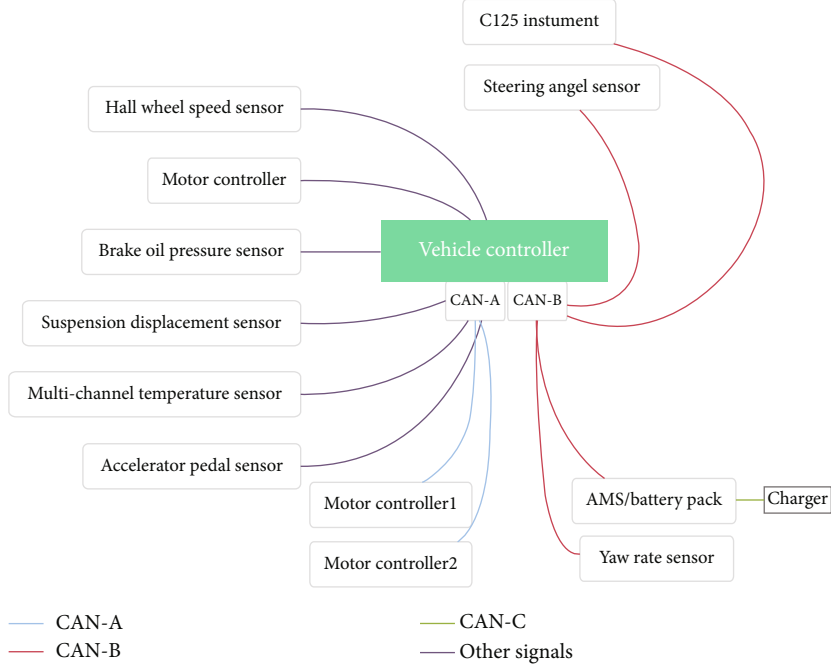


FIGURE 4: Vehicle CAN network.

### 3. Suspension System Data Analysis

The suspension system of this season's Gspeed formula E racing car is an independent suspension of unequal length, with a third spring system and a T-shaped anti-roll bar.

This part includes the calculation of roll gradient and roll stiffness, load transfer, and the analysis of shock absorber.

The purpose of suspension data analysis is to verify the design and guide the adjustment through the compilation and processing of the data. Detailed tuning projects consist of tire pressure, shock absorber gear, antiroll bar stiffness, load distribution of front and rear tires, adjusting four-wheel positioning parameters, and carrying out the corresponding fault troubleshooting.

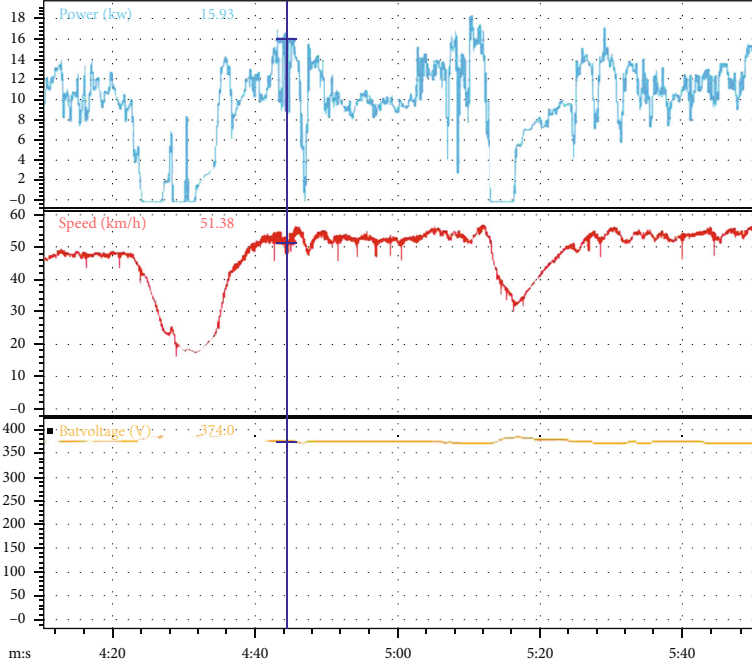


FIGURE 5: Reliability data template.

**3.1. Roll Gradient (RG) Analysis.** In vehicle dynamics, roll gradient refers to the roll angle of a vehicle per unit lateral acceleration.

Equation (1) is the definition formula of roll gradient RG.

$$RG = \frac{\alpha_{\text{roll}}}{G_{\text{lat}}}. \quad (1)$$

In the above formula,  $\alpha_{\text{roll}}$  is roll angle (deg);  $G_{\text{lat}}$  is lateral acceleration (g).

Therefore, in order to calculate the roll gradient, the first parameter we need to get is the roll angle. The following is the mathematical channel formula of the front and rear suspension roll angle  $\alpha_F$  and  $\alpha_R$  and the total suspension roll angle  $\alpha$ . In order to get the roll angle of the vehicle, the left and right suspension displacements should be calculated, and the trigonometric function formula should be used to solve the problem. Table 1 shows the vehicle parameters required by formulas (2)–(4).

$$\alpha_F = \text{ArcTan} \left[ \frac{(x_{\text{SuspLF}} - x_{\text{SuspRF}}) MR_F}{T_F} \right] \cdot \frac{180}{\pi}, \quad (2)$$

$$\alpha_R = \text{ArcTan} \left[ \frac{(x_{\text{SuspLR}} - x_{\text{SuspRR}}) MR_R}{T_R} \right] \cdot \frac{180}{\pi}, \quad (3)$$

$$\alpha = \text{ArcTan} \left[ \frac{(x_{\text{SuspLF}} - x_{\text{SuspRF}}) MR_F + (x_{\text{SuspLR}} - x_{\text{SuspRR}}) MR_R}{T_F + T_R} \right] \cdot \frac{180}{\pi}. \quad (4)$$

Among these parameters, suspension displacement is what we should detect. It can be obtained by measuring the

displacement of the shock absorber with the traditional linear displacement sensor. And when the suspension arrangement style is not suitable for using displacement sensor (for instance, a decoupling suspension with single spring mounted between two rockarms), we can use angular displacement sensor to get suspension displacement indirectly by measuring rockarm rotation angle. The angle and the suspension displacement usually have high linearity, whose linear coefficient can be fitted by means of parallel wheel jump simulation in Adams-Car [2]. After this work, what we need to do is to set up math channel in MoTec i2. Figure 6 shows the template of suspension system roll angle data.

It should be noted that the roll angle calculated from the suspension displacement is only the roll angle caused by the lateral transfer of sprung mass, that is, the suspension roll angle. Therefore, the following calculation is also the roll gradient of the suspension system using the roll angle of the suspension.

Then, we create a scatter graph with the vertical axis as roll angle and the horizontal axis as lateral acceleration and obtain the trend line equation, whose slope is the roll gradient of the suspension system. Figure 7 is the roll gradient diagram of GspeedE-2019 in a test. From the equations in the lower left corner of each template in the figure, it can be seen that the roll gradients of front suspension, rear suspension, and total suspension are  $0.552^\circ/\text{G}$ ,  $0.557^\circ/\text{G}$ , and  $0.555^\circ/\text{G}$ , respectively.

**3.2. Roll Stiffness.** The roll stiffness of suspension refers to the total elastic recovery couple moment given by the suspension system to the carriage under the unit carriage rotation angle when the vehicle rolls (the wheels remain on the ground). The roll stiffness of the suspension will affect the lateral load transfer of the car during steering and then affect the wheel

TABLE 1: Parameters in formulas (2)–(4).

Parameter	Description
$x_{\text{SuspLF}}$	Left front suspension displacement
$x_{\text{SuspRF}}$	Right front suspension displacement
$x_{\text{SuspLR}}$	Left rear suspension displacement
$x_{\text{SuspRR}}$	Right rear suspension displacement
$\text{MR}_F$	Front suspension motion ratio
$\text{MR}_R$	Rear suspension motion ratio
$T_F$	Front track width
$T_R$	Rear track width

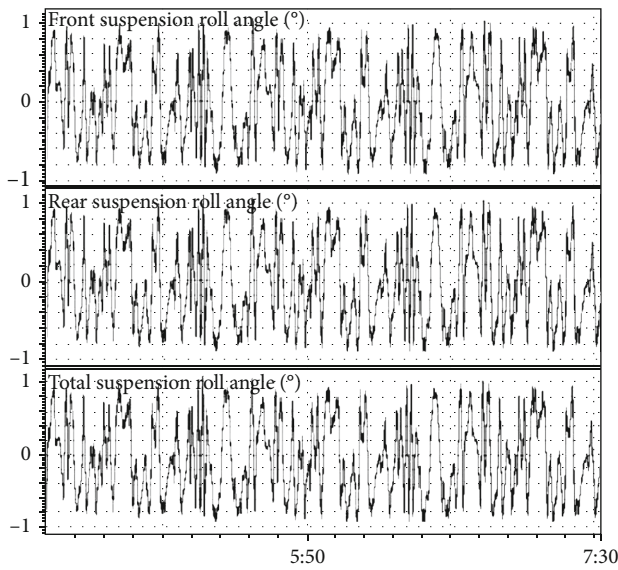


FIGURE 6: Template of suspension system roll angle data.

load of the inside and outside wheels as well as the front and rear wheels. The difference of wheel load will lead to the difference of the slip angle of the tires and then affect the steering characteristics [4]. According to the above roll gradient analyzed by MoTec i2 software and the vehicle parameters provided in Table 2, the roll stiffness of the suspension system and its components can be further calculated. Among them, the collection and analysis result of the roll gradient is  $\text{RG}_F = 0.552^\circ/\text{GRG}_R = 0.557^\circ/\text{G}$   $\text{RG} = 0.555^\circ/\text{G}$ .

We can obtain the following parameters by taking the torque on the ground:

Height of sprung mass center  $h_S$ :

$$h_S = \frac{W_T h - W_{UF}R_F - W_{UR}R_R}{W_S}. \quad (5)$$

Roll moment lever arm  $h_{\text{RM}}$ :

$$h_{\text{RM}} \cong h_S - [Z_F + (Z_R - Z_F)(1 - a_S)] = 0.252\text{m}. \quad (6)$$

Roll moment per lateral acceleration  $M_\phi$ :

$$M_\phi = W_S h_{\text{RM}}. \quad (7)$$

Then, the total suspension roll stiffness  $K_\phi$  is

$$K_\phi = \frac{M_\phi}{\text{RG}} = 1161.379\text{N} \cdot \text{m}^\circ. \quad (8)$$

According to the distribution of front and rear roll stiffness, the front and rear suspension roll stiffness  $K_{\phi F}$  and  $K_{\phi R}$  can be calculated as follows:

$$K_{\phi F} = K_\phi \cdot \frac{\text{RG}_R}{\text{RG}_F + \text{RG}_R} = 583.308\text{N} \cdot \text{m}^\circ, \quad (9)$$

$$K_{\phi R} = K_\phi - K_{\phi F} = 578.072\text{N} \cdot \text{m}^\circ. \quad (10)$$

Because in many cases, the roll stiffness provided by the spring cannot meet the requirement, so the antiroll bar mechanism is added. Therefore, suspension roll stiffness is the sum of the roll stiffness provided by spring and antiroll bar. Table 3 shows the vehicle parameters required by formulas (11) and (12).

$$K_{\phi F} = K_{\text{SpringF}} + K_{\text{ARBF}}, \quad (11)$$

$$K_{\phi R} = K_{\text{SpringR}} + K_{\text{ARBR}}. \quad (12)$$

In the above formula,  $K_{\text{SpringF}}$  ( $\text{N} \cdot \text{m}^\circ$ ) is the roll rate of the front spring;  $K_{\text{SpringR}}$  ( $\text{N} \cdot \text{m}^\circ$ ) is the roll rate of the rear spring;  $K_{\text{ARBF}}$  ( $\text{N} \cdot \text{m}^\circ$ ) is the roll rate of the front antiroll bar;  $K_{\text{ARBR}}$  ( $\text{N} \cdot \text{m}^\circ$ ) is the roll rate of the rear antiroll bar.

After calculating the roll stiffness of the spring through the known number of spring pounds, the roll stiffness of the antiroll bar can be further calculated [5].

By comparing the roll gradient and roll stiffness with the design objective, the gap between the actual race car and the simulation design can be obtained. If there is a large error, it is necessary to examine the specific cause of the error (for example, processing or assembly problem of parts) and solve it in time. In the test and tuning of real vehicle, after the ideal tuning strategy is obtained, the corresponding roll gradient can be used as the reference aim of the next season.

**3.3. Dynamic Vertical Load of Tires.** The vertical load directly affects the grip performance of the tire, while the load distribution between front and rear affects the steering characteristics of the car. In addition, the amount of tire load transfer can also affect the aerodynamic performance of the car. Therefore, knowing the tire dynamic vertical load is beneficial to evaluating the balance of a racing car, as well as the choice of tire pressure and analysis of tire surface temperature. By optimizing the four-wheel positioning parameters and other tuning methods, the tire load transfer of the racing car can be reduced

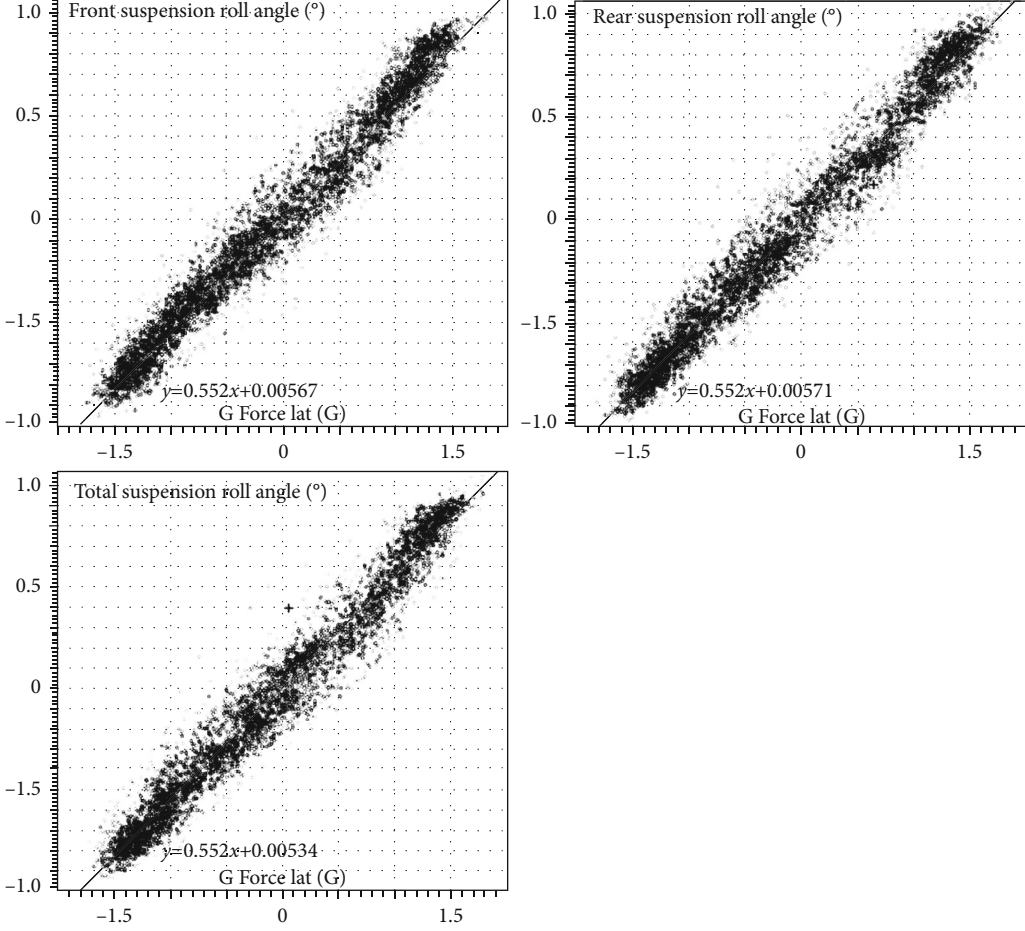


FIGURE 7: Roll gradient data template.

TABLE 2: Basic parameters of racing car.

Parameter	Description	Value : front	Rear	Total
$W_T$	Total mass (kg)	134.2	170.8	305
$W_U$	Unsprung mass (kg)	21	23	44
$W_S$	Sprung mass (kg)	113.2	147.8	261
$h$	Height of mass center (m)		0.28	
$Z$	Height of roll center (m)	0.03	0.04	
$R$	Tire load radius (m)	0.235	0.235	
$T$	Track width (m)	1.266	1.241	
$L$	Wheel base (m)		1.575	
$a_S$	Sprung mass distribution on the front suspension (%)		45	

TABLE 3: Parameters in formulas (11) and (12).

Parameter	Description
$K_{\text{SpringF}}$	Roll rate of the front spring
$K_{\text{SpringR}}$	Roll rate of the rear spring
$K_{\text{ARBF}}$	Roll rate of the front antiroll bar
$K_{\text{ARBR}}$	Roll rate of the rear antiroll bar

and balanced as far as possible, and the ultimate performance of race car can be further improved.

In order to calculate the dynamic vertical load of each wheel, it is necessary to understand the various parameters and influencing factors involved. And Figure 8 shows each component of wheel load.

The vertical load on each wheel is the sum of the components listed above. The detailed analysis and calculation are as follows.

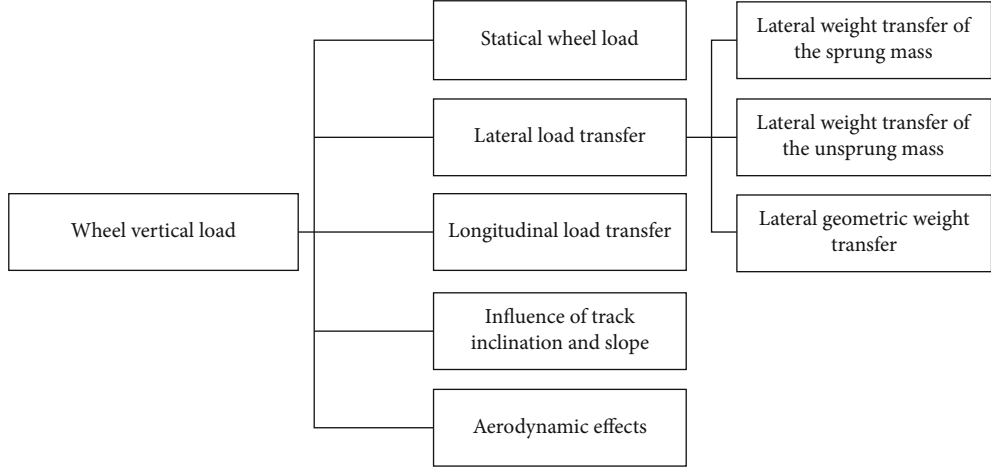


FIGURE 8: Each component of wheel load.



FIGURE 9: Static wheel load measurement.

**3.3.1. Static Wheel Load.** We can measure the static load of each wheel when the car is in the ready state (that is, the car with fully equipped driver). Figure 9 shows static wheel load measured by loadometer.

**3.3.2. Lateral Load Transfer.** We can measure the force of the suspension push rod through the pull pressure sensor, and then we can get the curve of tire load change with time. After that, by using the mechanical formula to calculate the other force elements of the suspension system, we can get the value of the downward pressure produced by the aerodynamic package on the race car, which is conducive to the design of the aerodynamic package on the racing car. Figure 10 shows the data collected by the pressure sensor.

(i) Lateral load transfer of the unsprung mass  $\Delta W_u$

$$\Delta W_{uF} = \frac{W_{uF} \cdot G_{lat} \cdot R_F}{T_F}, \quad (13)$$

$$\Delta W_{uR} = \frac{W_{uR} \cdot G_{lat} \cdot R_R}{T_R}. \quad (14)$$

It should be noted that in the early design, we used the tire load radius as an approximate value of unsprung mass center height. After the design work is completed, the height of wheel carrier mass center can be calculated in the 3D modeling software, which can be used as a more accurate value of unsprung mass center height.

(ii) Lateral geometric load transfer  $\Delta W_g$

$$\Delta W_{gF} = \frac{W_{sF} \cdot G_{lat} \cdot Z_F \cdot (S/L)}{T_F}, \quad (15)$$

$$\Delta W_{gR} = \frac{W_{sR} \cdot G_{lat} \cdot Z_R \cdot (1 - S/L)}{T_R}. \quad (16)$$

In the above formula,  $S$  is the distance (m) from the geometric center of rear axle to the sprung mass center in the side view. The calculation formula is as follows:

$$S = L \cdot \frac{W_{sF}}{W_s}. \quad (17)$$

It should be noted that the unsprung mass and the geometric load transfer cannot be measured by pull pressure sensor and displacement sensor. Except lateral acceleration, other parameters are in Table 1, considered as theoretical value.

(iii) Lateral load transfer of the sprung mass  $\Delta W_s$

$$\Delta W_{sF} = \frac{W_s \cdot G_{lat} \cdot h_{RM}}{T_F} \cdot q, \quad (18)$$

$$\Delta W_{sR} = \frac{W_s \cdot G_{lat} \cdot h_{RM}}{T_R} \cdot (1 - q). \quad (19)$$

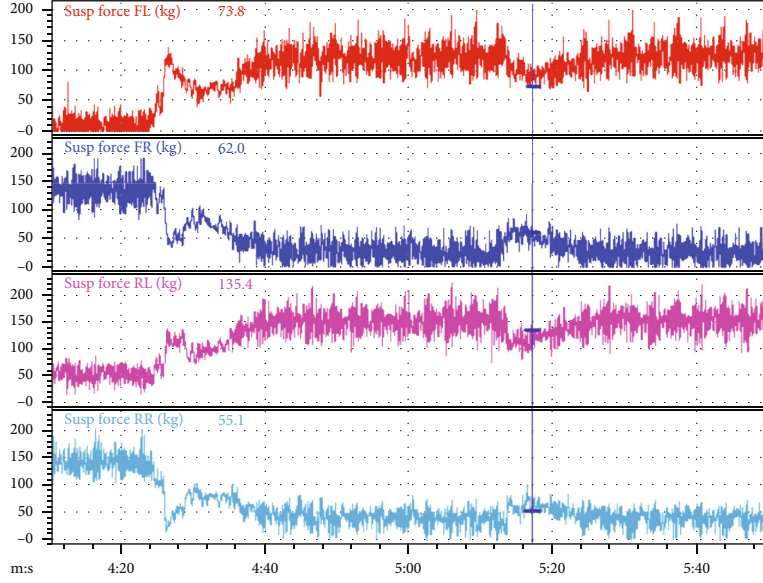


FIGURE 10: Data acquisition by pressure sensor.

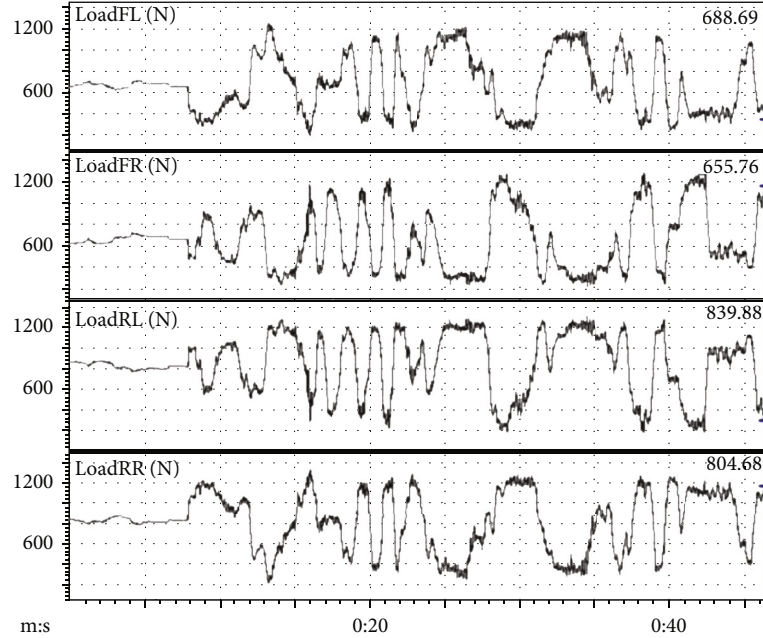


FIGURE 11: Tire dynamic load template.

The definition of  $q$  is

$$q = \frac{K_{\emptyset F}}{K_{\emptyset F} + K_{\emptyset R}} = \frac{RG_R}{RG_F + RG_R}. \quad (20)$$

From the above equations, we can see the importance of calculating roll gradient. The roll gradient can not only be used to further calculate the roll stiffness, verify whether the real car reaches the preliminary design expectation, and guide the adjustment of spring pounds and antiroll bar stiffness but also reflect the proportion of the lateral sprung mass

transfer on front and rear suspension compared with total amount and then calculate respective values.

### 3.3.3. Total Longitudinal Load Transfer $\Delta W_{Long}$

$$\Delta W_{Long} = \frac{W \cdot G_{Long} \cdot h}{L}. \quad (21)$$

To sum up, we can find that a large part of the calculation of load transfer is to calculate the value of mechanical concepts such as the mass center height, the roll center height, and the roll moment lever arm, while the lateral and

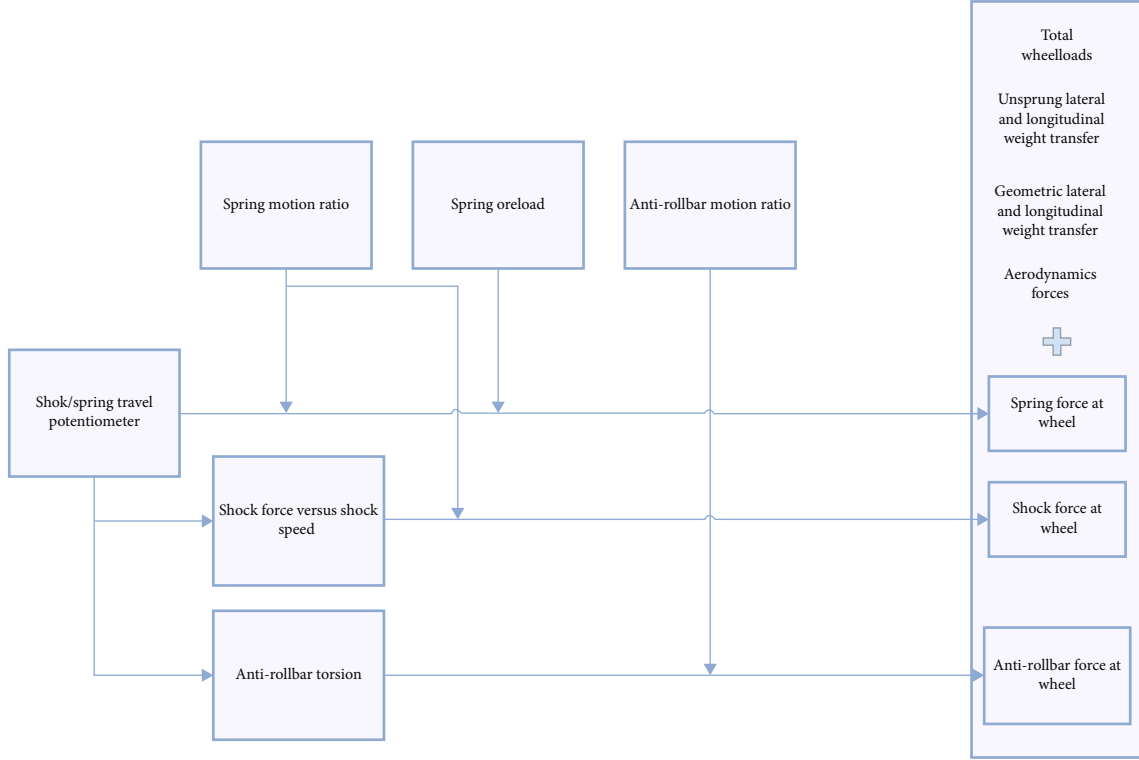


FIGURE 12: Tire load collection and calculation process.

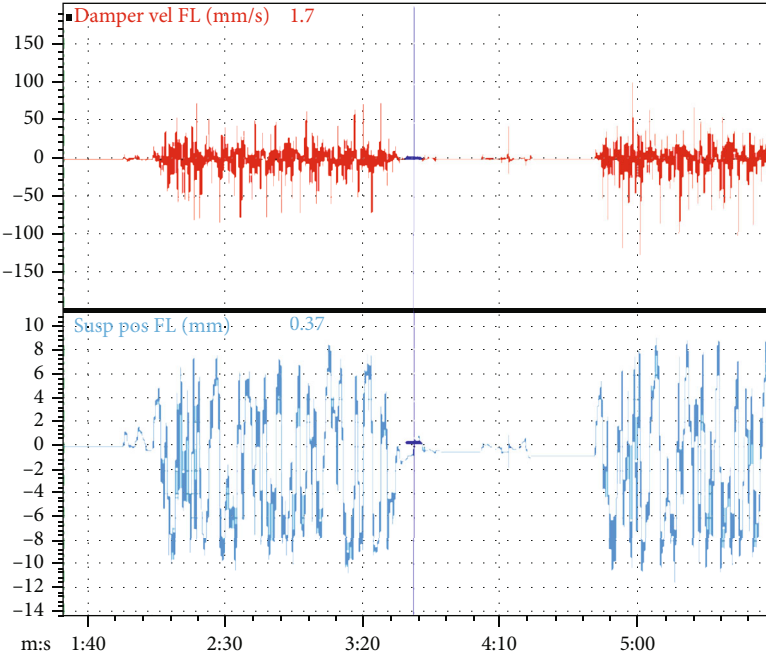


FIGURE 13: Displacement and velocity data acquisition diagram of shock absorber.

longitudinal accelerations are obtained by the digital acquisition equipment.

**3.3.4. Influence of Track Slope.** Since FSAE racing venues are usually well paved, this effect is ignored here. For example, the 2020 season was held at the Da'an Automotive Testing

Center in Xiangyang, Hubei Province, which is authorized by the National Automobile Testing Ground. As a result, road conditions can be guaranteed.

**3.3.5. Aerodynamic Effect.** The aerodynamic effect on car can be measured with relevant sensors. When all components are

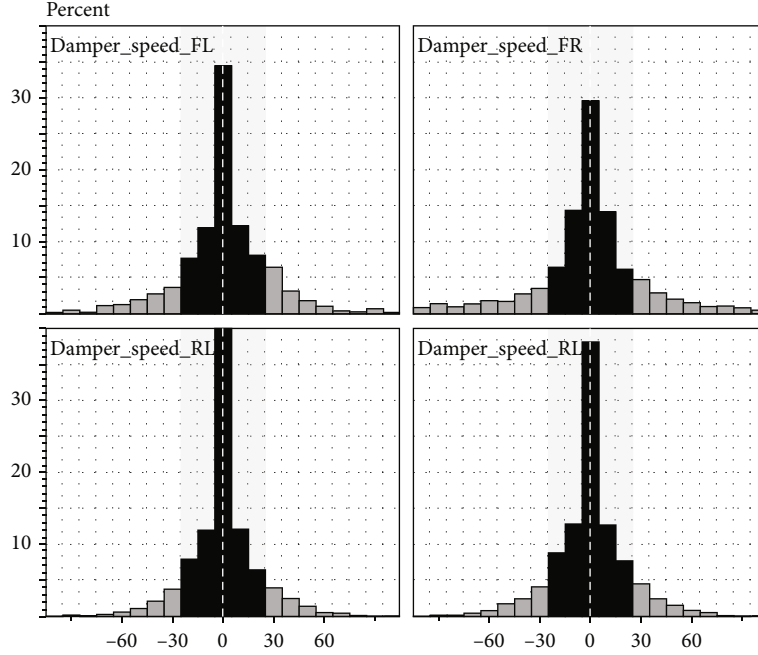


FIGURE 14: Damping velocity histogram data acquisition graph.

known, the total vertical load on each wheel can be calculated. Figure 11 is the dynamic load data of the tire in a skidpad track event (the skidpad track consists of two pairs of concentric circles in a figure of eight pattern) [3].

According to the average value in the upper right corner of the tire load graph above, the load transfer in the skidpad test is distributed as the front 48% and the rear 52%. Theoretically, neutral steering occurs when the distribution of load transfer is equal to the distribution of axle load [1]. Since the axle load distribution of the real car is the front 45% and the rear 55%, it can be concluded that the steering characteristics of the car are very close to the neutral steering.

According to the tire dynamic load, we can also choose more appropriate tire pressure according to the tire file provided by manufacturer. In FSAE, the straight line acceleration, skidpad event, and autocross event are performed in cold tire conditions [3], so in these events, the tire pressure can be directly selected according to the tire load that required lateral and longitudinal acceleration determine, without extra consideration of the tire temperature influence. The collection and calculation processes of tire load are shown in Figure 12.

**3.4. Damper Analysis Study.** For the data acquisition and analysis system, the analysis of the shock absorber is mainly to analyze its velocity through the displacement sensor. Equation (22) is the relation between the damper force and its velocity.

$$F_{\text{dam}} = C \cdot v_{\text{dam}}. \quad (22)$$

In the above formula,  $F_{\text{dam}}$  is the force generated by shock absorber,  $C$  is the damper coefficient, and  $v_{\text{dam}}$  is the velocity of the shock absorber.



FIGURE 15: Position of tire temperature sensor.

To get the velocity, we can take derivative of the shock absorber displacement signal.

$$v_{\text{dam}} = \frac{d}{dt} s_{\text{dam}}. \quad (23)$$

And Figure 13 shows the displacement and velocity data acquisition diagram of shock absorber.

In part 2.1 we have discussed, the shock absorber can be measured by linear displacement sensor directly or calculated through rockarm rotation angle.

The velocity interval of the shock absorber is mainly divided into three parts:

- (i) *The First Interval (<5 mm/s).* The velocity in this area is mainly caused by friction in the suspension system

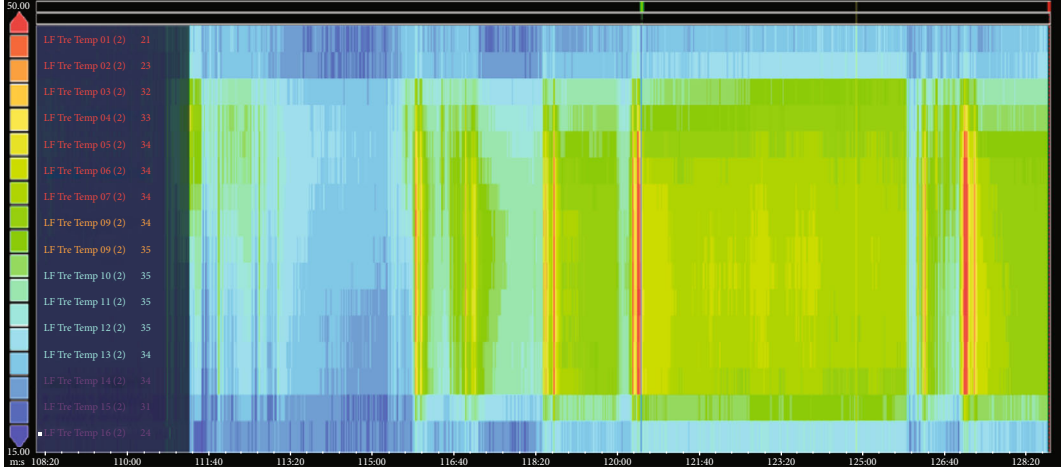


FIGURE 16: Tire temperature data acquisition graph.

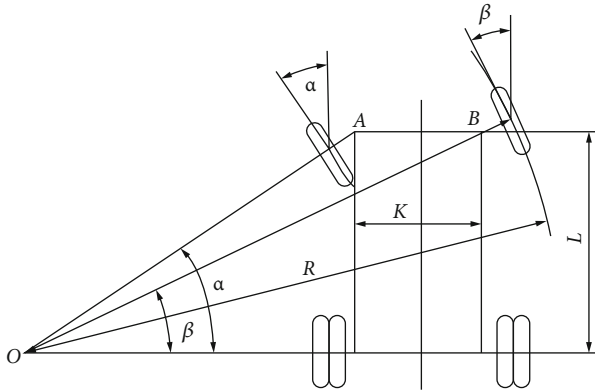


FIGURE 17: Ideal Ackermann angle.

- (ii) *The Second Interval (5-25 mm/s) (Low-Speed Damping Interval).* This area is the main area where the shock absorber responds to chassis motion of the car and is also an important area for driver to perceive the car
- (iii) *The Third Interval (25-200 mm/s) (High Speed Damping Interval).* The velocity of shock absorber in this area is mainly caused by road excitation. The impact of road shoulder usually allows the velocity to exceed 200 mm/s

In order to make the time ratio of shock absorber velocity in each interval more intuitive, damping velocity histogram, an important tool for damper analysis and adjustment, is presented here. The damping velocity histogram is a graph that describes the time proportion of damping in each velocity interval [6]. By observing the shape of the histogram, we can roughly analyze the “soft” and “hard” of the suspension. The establishment method of this histogram template is as follows: create a new workbench in MoTec i2, select the histogram template, and choose the time and proportion in horizontal and vertical coordinates, respectively. Finally, add the digital channel of the linear displacement sensor of the shock

absorber, import the data, and then generate the template [7]. Figure 14 shows the damping velocity histogram of the car after an endurance test.

In order to improve the tire grip performance and maintain a certain contact between tire and ground, the damping adjustment should make the histogram conform to the normal distribution as far as possible, and the histogram shape of the four wheels should be consistent with each other, as well as the difference between peak values should be as small as possible [2].

#### 4. Tire Temperature Analysis

As we know, tire surface temperature is an external indication of how well the tire works during testing. By analyzing the tire surface temperature and considering various factors of suspension kinematics and dynamics, the ideal working temperature range of the tire can be obtained, and the adjustment trend of tire camber can be deduced, as well as the real-time state of tire pressure in the test. By adding a tire temperature sensor, real-time tire temperature distribution and temperature rise data during running can be obtained conveniently, and the relationship between tire temperature and damping ratio can be established to guide the racing car set-up [8].

**4.1. Evaluate Wheel Camber from Tire Temperature.** As the car runs, the camber of wheels determines the position in which the tires are in contact with the ground, and the surface temperature of tires provides the desired position. When the car corners, for the outside wheels, by observing the color contrast diagram of tire temperature distribution, we can conclude that if the temperature distribution is uniform, then the camber angle is appropriate [9]. If the outer temperature of the outside wheel is significantly higher than that of the inner, it means that the camber angle is too small, otherwise, the camber angle is too large. For the inside wheel, if the temperature in the inner or middle of the wheel rises too fast, it means that the camber angle is too large; otherwise, it is too small. Since the outside wheels provide most of the lateral

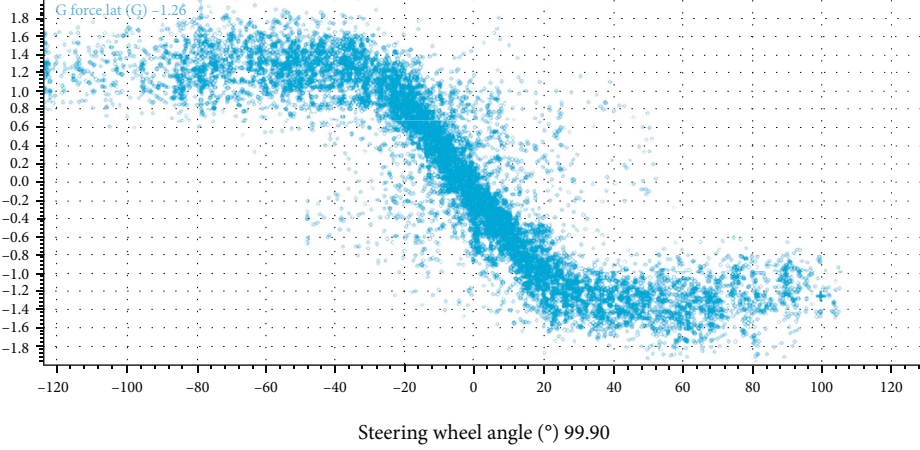


FIGURE 18: Data acquisition of steering wheel angle and lateral acceleration data scatter diagram.

TABLE 4: Parameters in formulas (26)–(28).

Parameter	Description
$\theta_{sw}$	Actual steering angle
$i$	Steering ratio
$L$	Lateral acceleration
$G_{la}$	Roll rate of the rear antiroll bar
$V$	Vehicle speed

force when cornering, the camber of the outside wheels is of more concern. We can characterize the camber state by the temperature difference between the inside and outside of the tire [10]. Equation (24) is the calculation formula of temperature difference between inside and outside tire surface:

$$\Delta T_{t_i} = T_{t_i}(\text{in}) - T_{t_i}(\text{out}). \quad (24)$$

In the above formula,  $i$  is LF (left front wheel), RF (right front wheel), LR (left rear wheel), RR (right rear wheel),  $T_{t_i}$  (in) is the temperature of the inside of the tire ( $^{\circ}\text{C}$ ), and  $T_{t_i}$  (out) is the temperature of the outside of the tire ( $^{\circ}\text{C}$ ).

However, it is not in line with scientific principles to make a final judgment on the data of a few specific corners, so it is necessary to evaluate the data of the whole lap comprehensively [11]. By equipping multichannel tire temperature sensors, we can obtain real-time tire temperature distribution and temperature rise data during running conveniently. Therefore, the proper camber angle can be determined by observing the average tire surface temperature difference throughout the lap [12]. Figure 15 shows the layout of tire temperature sensor on our car.

**4.2. Examine Tire Pressure from Temperature Analysis.** Except evaluating whether the camber angle is appropriate, we also use the tire temperature to analyze the tire pressure when the car is running [13]. Comparing the temperature of the inner and outer part of the tire with the middle, we can find that when the tire pressure is too low, the inner

and outer tire temperature will be higher than that of the middle part, while when the tire pressure is too high, the situation will be opposite. Therefore, the tire pressure can be evaluated by the difference between the middle and the average inner and outer tire temperature [14]. This difference is denoted as  $\Delta T p_i$ .

$$\Delta T p_i = T_{t_i}(\text{mid}) - \frac{T_{t_i}(\text{in}) + T_{t_i}(\text{out})}{2}. \quad (25)$$

In the above formula,  $T_{t_i}(\text{mid})$  is the tire middle temperature ( $^{\circ}\text{C}$ ),  $T_{t_i}(\text{in})$  is the tire inside temperature ( $^{\circ}\text{C}$ ), and  $T_{t_i}(\text{out})$  is the tire outside temperature ( $^{\circ}\text{C}$ ). When the result  $\Delta T p_i$  is positive, it indicates that the tire pressure is too high, vice versa. The following figure shows the tire temperature data collected in the first 20 seconds of a linear acceleration event. Through observation, it can be seen that the temperature in the middle part of the tire is higher and the temperature on both sides is lower. It can be preliminarily concluded that the tire pressure is too high and should be lowered. Figure 16 shows the tire temperature data acquisition graph.

## 5. Steering System Data Analysis

The design of the steering system is based on Ackerman steering geometry and takes the slip angle of tire into account. In the analysis of steering data, the steering characteristic of the race car is mainly studied. In addition, the steering design of Formula One should not only reduce tire wear and prolong the service life of tires but also have good steering stability [7]. The racing car mostly uses the broken steering trapezoid, the steering torque on the steering wheel from the transmission mechanism to the gear of the steering machine, and then driven by the gear and rack movement. Both ends of the steering rod are, respectively, connected with the steering rack and the steering knuckle arm. Under the action of the pull rod thrust and tension, the steering knuckle arm drives the tire to rotate, so as to achieve steering. A reasonable steering trapezoid structure should make the four steering wheels roll as far as possible without

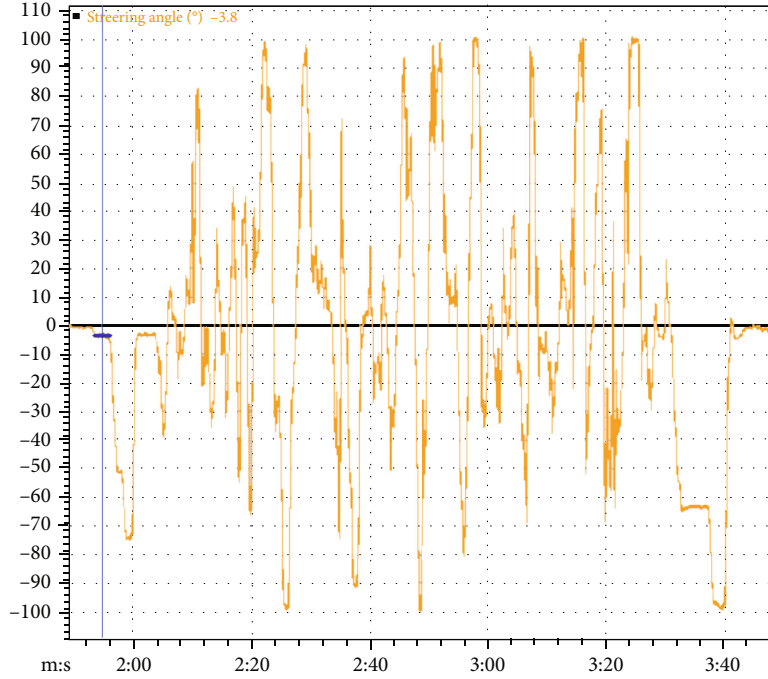


FIGURE 19: Actual steering angle data acquisition chart.

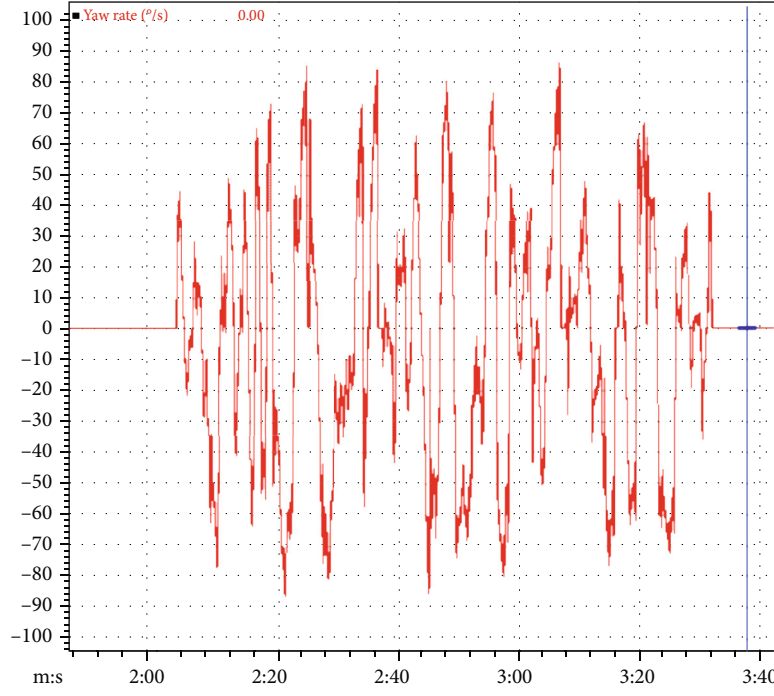


FIGURE 20: Yaw rate data acquisition graph.

sideslipping, that is, the instant center of the four steering wheels' speed intersects at the same point. When the rear wheels of the race car do not steer, the steering center of the race car should be on the rear wheel axle line. This steering relationship is the ideal Ackermann turning angle relationship, as shown in Figure 17. For this reason, the concepts of understeer angle and attitude angular velocity

are presented in this section to evaluate the steering characteristic of race cars [4]. Figure 18 shows the data acquisition of steering wheel angle and lateral acceleration data scatter diagram [15].

**5.1. Understeering Angle.** According to the definition of steering characteristic in Race Car Vehicle Dynamics [5], when

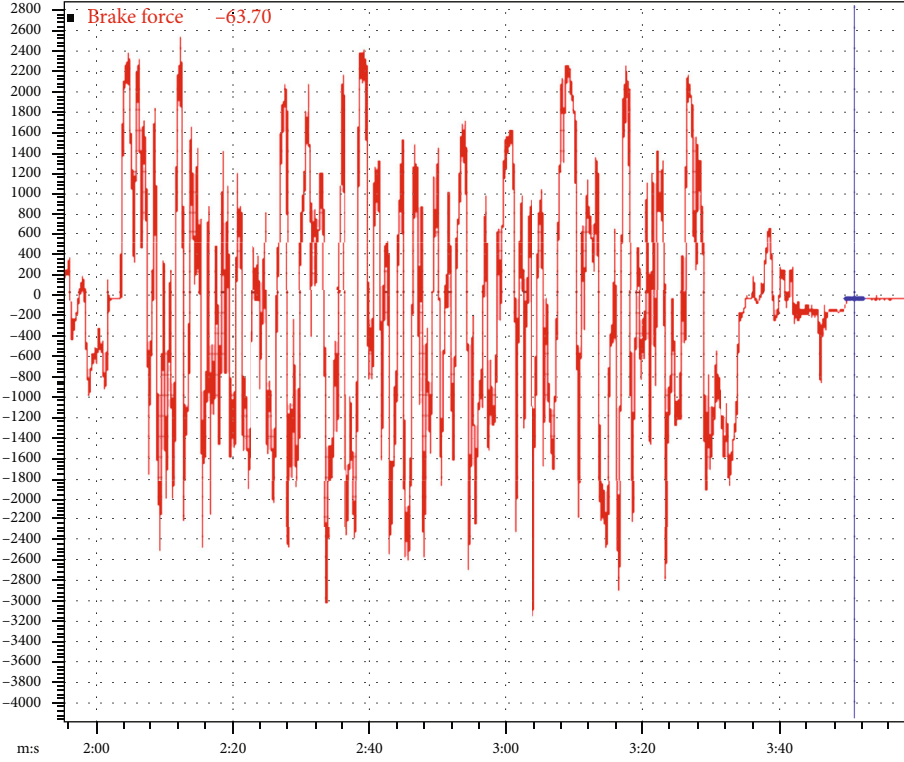


FIGURE 21: Braking force data collection in race car running test.

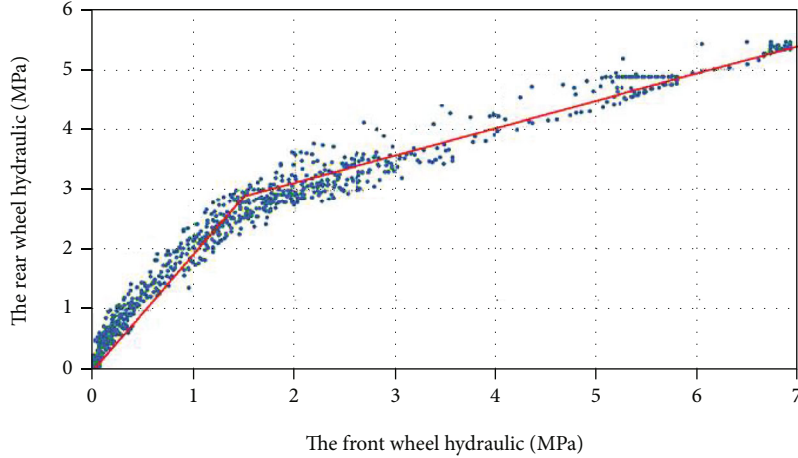


FIGURE 22: Actual braking force distribution obtained from data collection.

the actual wheel steering angle is equal to Ackerman steering angle, the vehicle will have neutral steering. When the steering angle is larger than Ackerman steering angle, the vehicle understeers. Oversteer on the other hand. Therefore, the difference between the absolute value of the actual wheel steering angle  $\theta$  and Ackerman steering angle  $\theta_{\text{Ack}}$  can be defined as the understeering angle  $\theta_u$ . The formula is as follows

$$\theta_u = |\theta| - |\theta_{\text{Ack}}|, \quad (26)$$

$$\theta = \frac{\theta_{sw}}{i}, \quad (27)$$



FIGURE 23: Race car running test.

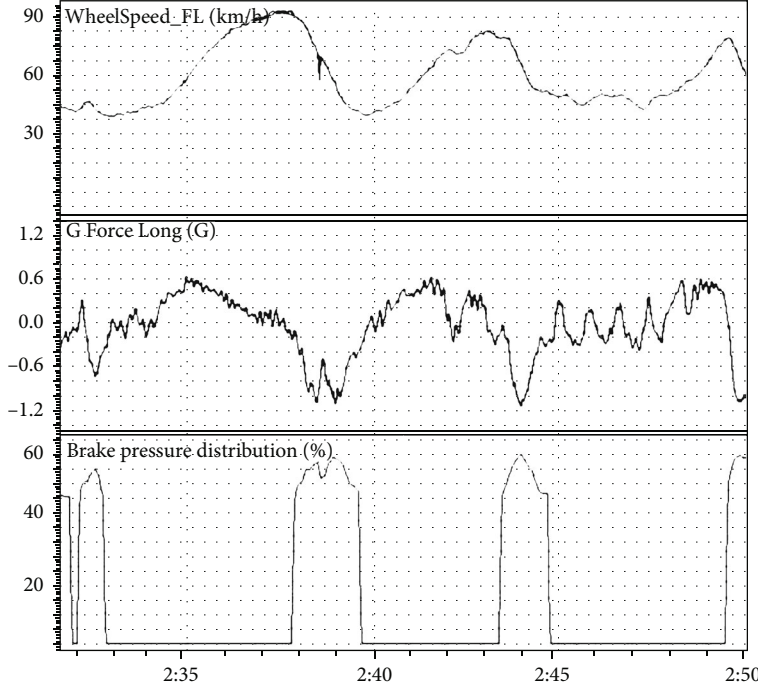


FIGURE 24: Brake data analysis template.

$$\theta_{\text{Ack}} = \frac{L \cdot G_{la}}{V^2}. \quad (28)$$

Table 4 shows the vehicle parameters required by formulas (26)–(28).

According to formula (26), the following conclusions can be drawn:

$$\theta_u \begin{cases} <0, \text{ oversteer}, \\ = 0, \text{ neutral steer}, \\ >0, \text{ understeer}. \end{cases} \quad (29)$$

By calculating the understeering angle, we can understand the steering characteristics at various stages of the corner. In order to study the overall steering characteristics of the car, the average understeering angle of the car can be obtained through the steady-state rotation test, and the overall steering characteristic of the car can be evaluated [13]. Figure 19 shows the actual steering angles of the car collected by MoTec i2 analysis.

**5.2. Attitude Velocity Analysis.** In addition to the understeering angle, the vehicle steering characteristics can be characterized by the difference between the absolute value of the actual yaw rate and the theoretical yaw rate, that is, the attitude angular velocity [16]. The following is the definition formula of attitude angular velocity  $\omega_a$ .

$$\omega_a = |\omega_{\text{yaw}}| - |\omega_t|, \quad (30)$$

$$\omega = \frac{G_{\text{lat}}}{V}. \quad (31)$$

In the above formula,  $\omega_{\text{yaw}}$  is the actual yaw rate of the vehicle ( $^{\circ}/s$ ), and  $\omega_t$  is the theoretical yaw rate of the vehicle ( $^{\circ}/s$ ). Figure 20 shows the yaw rate data collected.

Through the analysis, the following conclusions can be drawn:

$$\omega_a \begin{cases} <0, \text{ oversteer}, \\ = 0, \text{ neutral steer}, \\ >0, \text{ understeer}. \end{cases} \quad (32)$$

## 6. Braking System Data Analysis

In race car competition, we know that if you spend less time slowing down, you spend more time accelerating and you can improve your lap speed. As for the braking system, the important analysis data include vehicle speed, wheel speed, longitudinal acceleration, front and rear brake pressure, and front brake ratio.

**6.1. Braking Force.** The real braking force data can be collected through the brake oil pressure sensor, and the maximum longitudinal deceleration obtained in the running test corresponds to the maximum braking force of the car. The maximum braking force is one of the evaluation parameters of car braking performance, and usually, the maximum longitudinal deceleration of the car should be about 95% of the maximum lateral acceleration [5]. Figure 21 shows the braking force data collected in a race car running test, and Figure 22 shows the actual braking force distribution obtained from data collection. We performed a dynamic test on the car. Figure 23 shows the picture taken during the test [17].

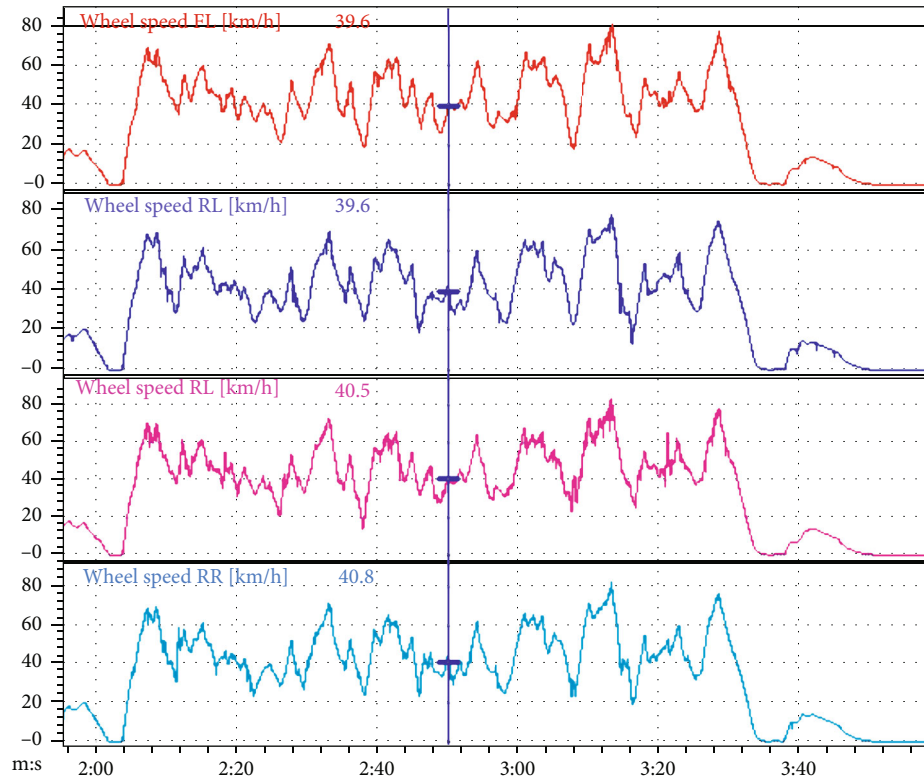


FIGURE 25: Wheel speed data.

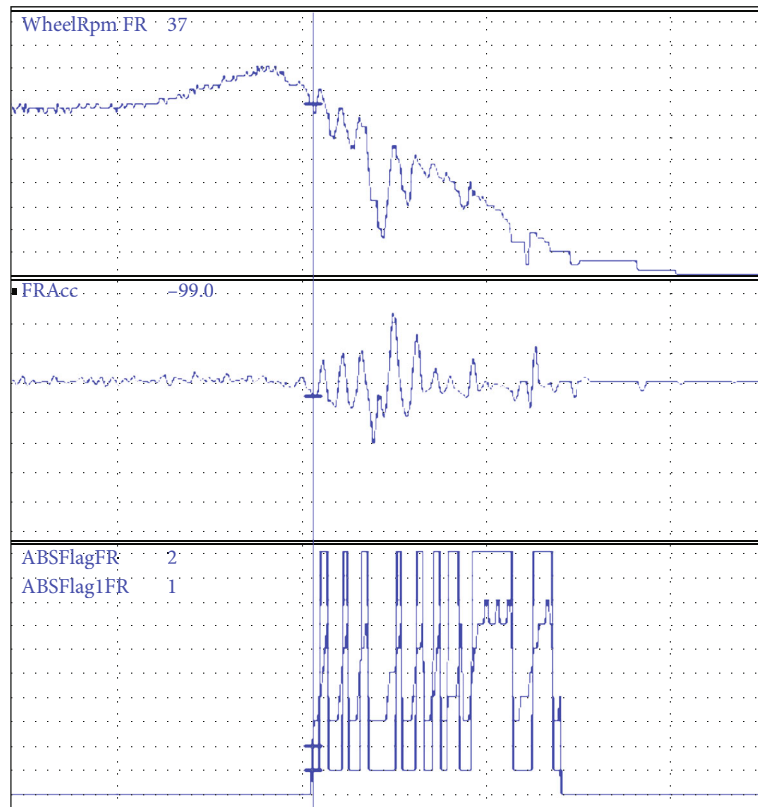


FIGURE 26: ABS simulation result.

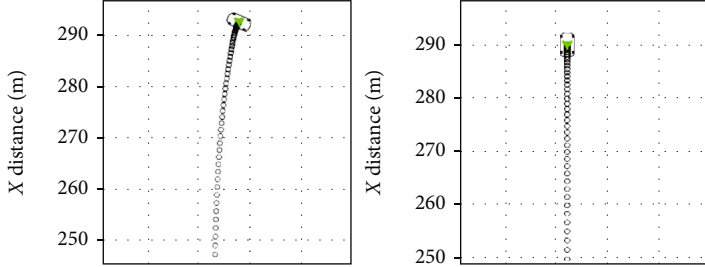


FIGURE 27: Comparison of simulation under open road conditions (the figure on the left does not include ABS braking, and the figure on the right includes ABS braking).

**6.2. Braking Lock.** The braking lock can be directly observed through the curve of wheel speed data. When decelerating, the wheel speed will drop in a straight line, when the tire is locked, the wheel speed will drop rapidly; when the driver senses that the tire is locked, he releases the brake slightly, and the wheel speed returns to its original straight line, forming a small trough, as shown in the wheel speed curve in Figure 24. The braking lock will cause the tire to lose grip performance, which should be avoided as far as possible.

**6.3. Braking Pressure Distribution.** Braking pressure distribution is the ratio of the front braking pressure to the total braking pressure, and equation (30) is the math channel formula of it:

$$B_F = \frac{\text{Brake}P_F}{\text{Brake}P_F + \text{Brake}P_R} \cdot 100\%. \quad (33)$$

In the equation,  $\text{Brake}P_F$  is the front brake pressure (MPa),  $\text{Brake}P_R$  is the rear brake pressure (MPa). Figure 25 shows the wheel speed data.

Braking pressure distribution affects the maximum braking force in the pure braking condition and the steering characteristics in the cornering condition with braking. Too much distribution of brake pressure on one axle will result in the corresponding tire lock. In the corner with braking, too much braking pressure to the front axle will lead to understeer, and too much to the rear axle will lead to oversteer. Therefore, according to the track characteristics and driver's feedback, and combined with data collection, we can improve the performance of our car by tuning braking pressure distribution properly.

**6.4. Set the ABS.** We analyze information obtained by data acquisition, concluding that in the process of race, the braking intensity is usually small and medium-sized. In the traditional brake system design, in order to make the front wheel lock first and achieve stable condition, the traditional design always matches a large synchronous adhesion coefficient to achieve this goal, so that will make the rear wheels have larger attachment loss. The inability to provide greater longitudinal adhesion of rear wheels results in the lack of lateral adhesion of the front wheels, which is very detrimental in the process of cornering and cannot guarantee the speed and stability of the car. Therefore, the ABS system is set to ensure that the front and rear wheels do not lock, lose steering ability,

or slip, and at the same time, the braking force distribution of the rear wheels is improved then the speed of cornering is improved. At the beginning of design, we use Simulink and Carsim cosimulation to establish the corresponding model, to judge its feasibility, and whether it can reduce the braking distance. Figure 26 shows the ABS/EBD simulation result, and Figure 27 shows the comparison of simulation under open road conditions [18].

## 7. Conclusion

This paper introduces the important mathematical channels for FSAE racecar data collection of the five types: reliability, suspension, tire, steering, and braking, as well as the corresponding calculation formula and the analysis template used in data analysis. Based on the MoTec i2 data processing platform, the paper carries out data analysis and post-processing for formula student. In addition, we use CAN bus communication to layout and design the vehicle sensor and wiring harness system.

In the sensor fault diagnosis, for CAN bus signal, we use interrupt counter counting method to diagnose the loss of signal frame or signal line disconnection and other faults.

As for reliability data, we analyze the safety and reliability of race cars by collecting battery voltage, battery temperature and motor power, so as to troubleshoot potential faults.

As for suspension system, we mainly analyzed the data collected by linear displacement sensor and studied the roll gradient, roll stiffness, tire load transfer, and shock absorber, so as to verify our design and tune the suspension to an appropriate state.

As for tires, we studied whether the corresponding four-wheel positioning parameters and tire pressure were appropriate and whether the utmost performance of tires could be exerted through the data collected from the multichannel tire temperature sensor.

As for the steering system, we obtained steering angle and lateral acceleration scatter diagram and change rate of steering angle and yaw velocity, to judge the steering characteristics of race car and make corresponding adjustments.

As for the braking system, we analyzed maximum braking force, braking pressure distribution, and checked wheel speed data to deal with brake lock. Furthermore, we do some research on the ABS/EBD system.

Due to our limited knowledge, the data analysis we have done is relatively basic, but for FSAE teams, it has been an

effective and systematic approach. We will continue to improve our data analysis method to make it more standardized in the future.

## Data Availability

Data sharing not applicable to this article as no datasets were generated or analyzed during the current study.

## Conflicts of Interest

The authors declared no potential conflicts of interest with respect to the research, authorship, and/or publication of this article.

## References

- [1] S. A. E. Formula2020, <http://www.formulastudent.com.cn/>.
- [2] Organizing Committee of Chinese Formula Student, *2019 Chinese Formula Student Racing Manual*, China Association of Automotive Engineers, Beijing, 2019.
- [3] G. Zhang, *Design and Adjustment of FSAE Racing Suspension*, Tongji University, Shanghai, 2017.
- [4] J. Segers, *Analysis Techniques for Racecar Data Acquisition Second Edition*, SAE International, 2014.
- [5] W. F. Milliken and D. L. Milliken, *Race Car Vehicle Dynamics*, Warrendale SAE, 1995.
- [6] Y. Peng and Z. Deng, “Design and development of data acquisition system based on FSAE,” *Electronic Technology and Software Engineering*, vol. 3, no. 3, pp. 163–165, 2019.
- [7] C. Huang, Y. Zhou, and X. Song, “Design of steering data acquisition system for FSAE racing car,” *Equipment Manufacturing Technology*, vol. 8, pp. 96–99, 2018.
- [8] Q. Yue, Q. Wei, and X. Ren, “Research and design of FSAE racing car data acquisition system,” *Modern Electronic Technology*, vol. 41, no. 5, pp. 69–73, 2018.
- [9] Z. Deng, C. Xu, and B. Wang, “Design of FSAE racing suspension data acquisition system based on LabVIEW,” *Journal of Hefei University of Technology (Natural Science Edition)*, vol. 38, no. 8, pp. 1018–1022, 2015.
- [10] D. Harsh and B. Shyrokau, “Tire model with temperature effects for formula SAE vehicle,” *Applied Sciences*, vol. 9, no. 24, p. 5328, 2019.
- [11] A. Ayyad and M. Fathizadeh, “Telemetry and data collection to improve formula SAE car,” in *World Congress on Engineering and Computer Science, WCES 2017*, San Francisco, CA, 2017.
- [12] SAE International, *2020 Formula SAE Rules*, 2020, April 2020, <http://students.sae.org/cds/formulaseries/ryles/>.
- [13] G. Xiang, *Automotive Engineering II*, Mechanical Industry Press, Beijing, 2013.
- [14] E. M. Kasprzak and D. Gentz, “The formula SAE tire test consortium-tire testing and data handling,” in *Motorsports Engineering Conference and Exhibition SAE International*, Dearborn, Michigan, 2016.
- [15] B. Chen, Y. Liu, and W. Shi, “Optimization design and virtual prototype modeling and simulation analysis of FSAE car steering trapezium,” in *2018 International Seminar on Computer Science and Engineering Technology*, Shang Hai, China, 2018.
- [16] A. Tokosch, D. Hake, K. Meah, and J. Maier, “Design and implementation of a drivetrain for an FSAE electric vehicle,” in *2019 IEEE International Conference on Environment and Electrical Engineering and 2019 IEEE Industrial and Commercial Power Systems Europe (EEEIC/I&CPS Europe)*, Genova, Italy, 2019.
- [17] J. Zhang, X. Lv, and Y. Lv, “Research on vehicle control strategy and hardware in loop for pure electric FSAE vehicle,” in *The 2nd International Seminar on Computer Science and Engineering Technology (SCSET) 2020*, Shanghai, China, 2020.
- [18] R. Luca, V. Giovanni, B. Alessandro, F. Lorenzo, and F. Giovanni, “Optimization of the performance of a formula SAE engine by means of a wastegate valve electronically actuated,” *Energy Procedia*, vol. 101, pp. 654–661, 2016.